Nanosize Silicon Whiskers Produced by Chemical Vapor Deposition: Active Getters for NF_3

Lu Shen,[†] Youming Xiao,[†] Elizabeth Vileno,[†] Ying Ma,[†] Steven L. Suib,*[,†,‡,§] Francis S. Galasso,[†] James D. Freihaut,[⊥] and Steven J. Hardwick[∥]

U-60, Department of Chemistry, Department of Chemical Engineering, and Institute of Materials Science, University of Connecticut, Storrs, Connecticut 06269-3060; United Technologies Research Center, Silver Lane, East Hartford, Connecticut 06108; and Novapure Corp., 7 Commerce Drive, Danbury, Connecticut 06810

Received December 20, 1994. Revised Manuscript Received February 23, 1995[⊗]

Nanosize whiskers on the order of 120 Å in diameter have been prepared by chemical vapor deposition reactions of methyltrichlorosilane and H_2 carrier gas on porous silica (Davisil) and other supports. The porosity and composition of the support control the resultant size of the Si whiskers. NaY zeolite and C supports also allow formation of Si whiskers, however, silica gel leads to formation of spherical deposits of Si on the order of 5 μm. X-ray powder diffraction and line broadening methods show that the whiskers are crystalline and are small particles. X-ray photoelectron spectroscopy shows the presence of elemental Si in the CVD systems. Surface area measurements of the supports before and after CVD suggest that the pores of the support are still accessible after formation of Si whiskers. The Si whiskers on various supports have been used as outstanding getters for decomposition of NF_3, a toxic gas which is used as an etchant for cleaning Si wafers in the semiconductor industry.

Introduction

Synthesis, characterization and applications of submicrometer (100 nm to 1 mm) and nanoscale (1–100 nm) particles have received tremendous attention in recent years.[1-5] Submicrometer and nanoscale particles have found applications in catalysis,[6] ceramics,[7] electronics,[8] optical devices,[9] photography,[10] and semiconductor technology.[11] For example, nanophase titania (TiO_2) is much more active at removing sulfur contaminants than more conventional forms of TiO_2.[12] Ceramic nanophase materials are more ductile than traditional ceramics at low temperatures.[13] Nanophase metals can also be used to enhance mechanical strength.[14]

Quantum dots and wells made of such nanophase materials can be used to control the movement of single electrons.[15] Optoelectronic devices of nanophase particles are continuing to be pursued with the hope that lasing materials can be reproducibly produced and operated to selectively illuminate nanoareas and create nanostructures in order to control information flow.[16] Latent images in the photographic processes are believed to entail the creation of a 4 atom Ag cluster.[17] Potential applications of such nanophase materials are practically endless.

Nanophase materials can be prepared by a variety of methods including metal atom vaporization,[18] sol–gel,[19] solvated metal atom dispersion,[20] chemical vapor deposition,[21] mechanical milling,[22] molecular beam,[23] self-assembly,[24] Langmuir–Blodgett,[25] plasma,[26] and other methods. Each of these methods has various advan-

[†] Department of Chemistry.
[‡] Department of Chemical Engineering.
[§] Institute of Materials Science.
[⊥] United Technologies Research Center.
[∥] Novapure Corp.
* To whom correspondence should be addressed.
[⊗] Abstract published in *Advance ACS Abstracts,* April 1, 1995.

(1) Bodker, F.; Morup, S.; Linderoth, S. *Phys. Rev. Lett.* **1994**, *72*, 282–285.
(2) Puvvada, S.; Baral, S.; Chow, G. M.; Qadri, S. B.; Ratna, B. R. *J. Am. Chem. Soc.* **1994**, *116*, 2135–2136.
(3) Eastman, J. A. *J. Appl. Phys.* **1994**, *75*, 770–779.
(4) Ruoff, R. S.; Lorents, D. C.; Chan, B.; Malhotra, R.; Subramoney, S. *Science* **1993**, *259*, 346–348.
(5) Labeau, M.; Gautheron, B.; Cellier, F.; Valletregi, M.; Garcia, E.; Calbet, J. M. G. *J. Solid State Chem.* **1993**, *102*, 434–439.
(6) (a) Zhao, J.; Huggins, F. E.; Feng, Z.; Lu, F. L.; Shah, N.; Huffman, G. P. *J. Catal.* **1993**, *143*, 499–509. (b) Hutton, R. D.; Pocard, N. L.; Alsmeyer, D. C.; Schueller, O. J. A.; Spontak, R. J.; Huston, M. E.; Huang, W. H.; McCreery, R. L.; Neenan, T. X.; Callstrom, M. R. *Chem. Mater.* **1993**, *5*, 1727–1738.
(7) Ellis, D. E.; Guo, J.; Lam, D. J. *J. Am. Ceram. Soc.* **1994**, *77*, 398–403.
(8) (a) Bein, T. *Nature* **1993**, *361*, 207–208. (b) Pickett, C. J.; Ryder, K. S.; Moutet, J. C. *J. Chem. Soc., Dalton Trans.* **1993**, *24*, 3695–3703.
(9) (a) Carts, Y. A. *Laser Foc. World* **1993**, *29*, 43–44. (b) Curtis, C. L.; Doan, V. V.; Credo, G. M.; Sailor, M. J. *J. Electrochem. Soc.* **1993**, *140*, 3492–3494.
(10) Serpone, N.; Lawless, D.; Lenet, B. *J. Imaging Sci. Technol.* **1993**, *37*, 517–523.
(11) (a) Zhou, H. S.; Honma, I.; Komiyama, H.; Haus, J. W. *J. Phys. Chem.* **1993**, *97*, 895–901. (b) Cassagneau, T.; Hix, G. B.; Jones, D. J.; Mairelestorres, P.; Rhomari, M.; Roziere, J. *J. Mater. Chem.* **1994**, *4*, 189–195.
(12) Dagani, R. *Chem. Eng. News* **1993**, *Mar. 22*, 20.
(13) Karch, J.; Birrenger, I.; Gleiter, H. *Nature* **1987**, *330*, 556–558.
(14) Gertsman, V. Y.; Birringer, R.; Valiev, R. Z.; Gleiter, H. *Scr. Met. Mater.* **1994**, *30*, 229–234.
(15) (a) Chemesddine, A. *Chem. Phys. Lett.* **1993**, *216*, 265–269. (b) Wang, L. W.; Zunger, A. *J. Phys. Chem.* **1994**, *98*, 2158–2165. (c) Bockelmann, U. *Phys. Rev. B–Condens. Matter* **1993**, *48*, 17,637–17,640.
(16) Poirier, G. E.; Hance, B. K.; White, J. M. *J. Phys. Chem.* **1993**, *97*, 6500–6503.
(17) (a) Williams, D. B., Pelton, A. R., Gronsky, R., Eds. *Images of Materials*; Oxford University Press: New York, 1991. (b) Morton, R. A., Ed.; *Photography for the Scientist*; Academic Press: London, 1984.
(18) Utamapanya, S.; Klabunde, K. J.; Schlup, J. R. *Chem. Mater.* **1991**, *3*, 175–181.
(19) (a) Bourrell, D. J.; Kaysser, W. *J. Am. Ceram. Soc.* **1993**, *76*, 705–711. (b) Kurihara, L. K.; Suib, S. L. *Chem. Mater.* **1993**, *5*, 609–613.
(20) Klabunde, K. J.; Li, Y. X.; Tan, B. *Chem. Mater.* **1991**, *3*, 30–39.

0897-4756/95/2807-0961$09.00/0

tages and disadvantages depending on the specific area of research being investigated. Purity, unique structures, ease of preparation, reproducibility, and scaleup are some of the important factors to be considered in developing a synthetic procedure.

The interest in decomposition of NF_3 revolves around its use in the semiconductor industry for etching and cleaning of silicon,[27] tungsten,[28a] and tungsten silicide systems[28b] with formation of volatile fluoride species. NF_3 is also used to clean reactors[29a] and reactor chambers.[29b] NF_3 is used in combination with O_2 to increase the rate of oxidation of silicon[30a] and with H_2 to etch SiO_2.[30b]

The production of NF_3 has escalated in the past seven years, and current scrubbers for NF_3 operate at high temperatures (130–800 °C) and are expensive. Some scrubbers like activated carbon can decompose to form volatile fluorocarbons, which are environmentally hazardous.[27,31] Another common practice for decomposing NF_3 is combustion,[27] which produces HF and NO_x, further complicating disposal issues.

Some more recently proposed gettering systems involve the thermal decomposition of NF_3 over metals or supported metals, and other systems. The following systems have been reported to decompose NF_3: BN at 250–250 °C,[32] Si_3N_4 at >200 °C,[33] various metals and metalloids (Si, B, W, Mo, V, Se, Te, Ge) at temperatures of 200–800 °C,[34] Cu and Ni non-oxide compounds supported on activated carbon at 100–300 °C,[35] and metal oxides and activated carbon at 200–600 °C.[36]

Research reported here deals with the use of chemical vapor deposition (CVD) methods for the preparation of nanophase ultrafine Si whiskers on different porous substrates. These Si nanowhiskers are outstanding getters for the decomposition of NF_3. Synthesis, characterization, and NF_3 decomposition reactions will be discussed.

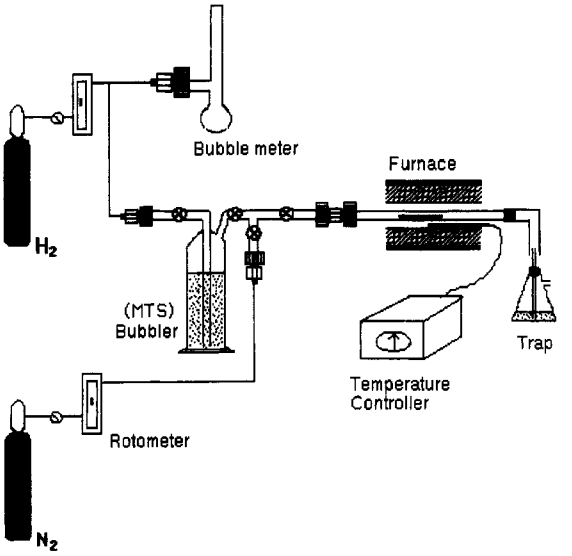

Figure 1. Apparatus used for CVD.

Table 1. X-ray Diffraction Line Broadening Data

substrate	diameter of whiskers[a]
Davisil	123
carbon	302
NaY	409

[a] In angstroms.

Experimental Section

Chemical Vapor Deposition. Methyltrichlorosilane (Aldrich, Milwaukee, WI) and H_2 (Matheson, NJ) were used as feed reactants to prepare Si nanowhiskers. Reaction conditions can be optimized to prepare either Si or SiC. A flow rate of 21–72 mL/min of H_2 gas was used. Methyltrichlorosilane was placed in a bubbler and kept at room temperature. Chemical vapor deposition was carried out at 1 atm in the reactor shown in Figure 1. N_2 gas was used in certain cases as a diluent. Porous substrates were placed in a furnace which was heated between 800 and 1050 °C during reaction. The deposition time was varied from 5 min to 1 h.

Various porous substrates were used such as Davisil silica gel (grade 646, 35–60 mesh, Aldrich, Milwaukee, WI), silica gel (28–200 mesh, Fischer Scientific, Fair Lawn, NJ, No. S-157), carbon (grade 20-SPD, BET = 22,00 m^2/g, Maxisorb, United Technologies Research Center, E. Hartford, CT), NaY (Alfa Ventron, Danvers, MA), and AlN powder (homemade). Powders were loaded into a quartz boat.

X-ray Diffraction. X-ray powder diffraction studies of the supports and the Si deposits were made with a Scintag Model PDS 2000 diffractometer interfaced to an IBM personal computer. Cu Kα radiation was used at a current of 40 mA and a beam voltage of 45 kV. Data were analyzed by comparison to a JCPDS file as well as by using standards. XRD data were analyzed with the Debye–Sherrer relationship to yield line broadening data such as those of Table 1.

Scanning Electron Microscopy. Scanning electron microscopy (SEM) studies were done in an AMRAY Model 1810 D instrument with an AMRAY PV 9800 energy-dispersive X-ray (EDX) analyzer accessory. Samples were analyzed without any coatings by minimizing the beam current and beam voltage and by signal averaging.

X-ray Photoelectron Spectroscopy. X-ray photoelectron spectroscopy (XPS) experiments were performed using a

(21) (a) Uno, T.; Kasuga, T.; Nakayaama, S.; Ikushima, A. J. *J. Am. Ceram. Soc.* **1993**, *76*, 539–541. (b) Shen, L.; Tan, B. J.; Willis, W. S.; Galasso, F. S.; Suib, S. L. *J. Am. Ceram. Soc.* **1994**, *77*, 1011–1016.
(22) Basset, D.; Matteazzi, P.; Miani, F. *Mater. Sci. Eng. A–Struct. Mat. Prop. Microstruct. Proc.* **1993**, *168*, 149–152.
(23) Singer, K. E.; Rutter, P.; Peaker, A. R.; Wright, A. C. *Appl. Phys. Lett.* **1994**, *64*, 707–709.
(24) Schönenberger, C.; Sondag-Huethorst, J. A. M.; Jorritsma, J.; Fokkink, L. G. J. *Langmuir* **1994**, *10*, 611–614.
(25) (a) Chow, G. M.; Markowwitz, M. A.; Singh, A. *J. Min Met. Mater. Soc.* **1993**, *45*, 62–65. (b) Wang, H. Y.; Lando, J. B. *Langmuir* **1994**, *10*, 790–796.
(26) (a) Davanloo, F.; Lee, T. J.; You, J. H.; Park, H.; Collins, C. B. *Surf. Coat. Technol.* **1993**, *62*, 564–569. (b) Smirnov, B. M. *Plasma Chem. Plasma Proc.* **1993**, *13*, 673–684. (c) Nam, S. S.; Iton, L. E.; Suib, S. L.; Zhang, Z. *Chem. Mater.* **1989**, *1*, 529–534.
(27) (a) Barkanic, J. A.; Hardy, T. K.; Shay, R. H.; Fukushima, H. Air Products and Chemicals, Inc., Allentown, PA, 1987. (b) Woytek, A.; Lileck, J. T. Barkanic, *J. Solid State Technol.* **1984**, *27*, 172–175. (c) Delfino, M.; Chung, B. C.; Tsai, W.; Salimian, S.; Favreau, D. P.; Merchant, S. M. *J. Appl. Phys.* **1992**, *72*, 3718–3725.
(28) (a) Hirase, I.; Petitjean, M. Eur. Pat. Appl. EP 382,986. CA 113: 194426p. (b) Lee, R. L.; Terry, F. L. *J. Vac. Sci. Technol. B* **1991**, *9*, 2747–2751.
(29) (a) Bruno, G.; Capezutto, P.; Cicala, G.; Manodoro, P. *J. Vac. Sci. Technol. A* **1994**, *12*, 690–698. (b) Langan, J. G.; Felker, B. S. *Proc. Electrochem. Soc.* **1992**, *92*, 135–144.
(30) (a) Morita, M.; Kubo, T.; Ishihara, T.; Hirose, M. *Appl. Phys. Lett.* **1984**, *45*, 1312–1314. (b) Yokoyama, S.; Yamakage, Y.; Hirose, M. *Appl. Phys. Lett.* **1985**, *47*, 389–391.
(31) Aramaki, M.; Nakagawa, S.; Nakano, H.; Ichimaru, H.; Tainake, M. Ger. Offen. DE 4,002,642 CA 114: 256690b.
(32) (a) Iwanaga, T.; Harada, I.; Aritsuka, M. Jpn. Kokai Tokkyo Koho, JP 02,245,223, Oct 1990; CA 114: 170384t. (a) Iwanaga, T.; Harada, I.; Aritsuka, M. Jpn. Kokai Tokkyo Koho, JP 02,265,620, Oct 1990; CA 114: 191644t.
(33) Kashiwada, K.; Hasumoto, T.; Torisu, J.; Konishi, M. Jpn. Kokai Tokkyo Koho, JP 04,225,818, Dec 1990; CA 118: 11036x.
(34) Aramaki, M.; Sakaguchi, H.; Suenaga, T.; Kobayashi, Y. Jpn. Kokai Tokkyo Koho, JP 61,204,025, Sept 1986; CA 106: 72242b.
(35) Kubo, M.; Nakagawa, S. Jpn. Kokai Tokkyo Koho, JP 05,192,-538, Aug 1993; CA 119: 187642b.
(36) Orihara, I.; Fukushima, M.; Sato, S. Jpn. Kokai Tokkyo Koho, JP 05,15,740, Jan 1993; CA 118: 260336r.

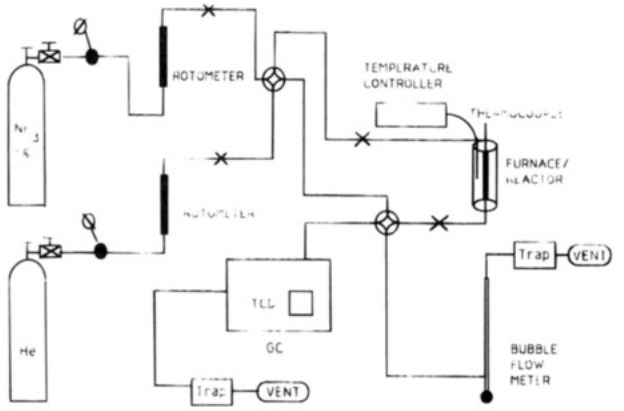

Figure 2. Apparatus used for NF_3 decomposition.

Leybold Heraeus spectrometer with an EA10 hemispherical analyzer. Mg Kα or Al Kα radiation was used at 600 W power (15 keV, 40 mA). The base pressure in the analysis chamber was 1×10^{9} Torr during data collection. Wide scans were collected at a pass energy of 178.25 eV from 0 eV to about 1250 eV binding energy to identify all elements on the surfaces of the Si deposited materials. High resolution or narrow scans were collected at a pass energy of 35.75 eV over selected regions to obtain more detailed information concerning oxidation states of the different surface elements. Samples were pressed into In foil in order to minimize charging effects.

Scanning Auger Microscopy. Scanning Auger microscopy studies were done on a PHI Model 6100 Auger spectrometer at a base pressure of 5×10^{-9} Torr. The spectrometer was equipped with a single-pass cylindrical mirror analyzer (CMA) with a coaxial electron gun. Auger electron spectra were recorded with an energy resolution of 0.6%. Samples were mounted on In foil in order to minimize charging effects.

Luminescence. Luminescence excitation and emission experiments were done on a double-monochromator Spex Model 2200 B spectrometer in the front face mode. Samples were loaded into quartz tubes and evacuated to eliminate quenching effects of oxygen. Emission and excitation slits were set at 1 nm to obtain high-resolution data. Excitation wavelengths were varied in order to clearly identify absorption bands and related emission bands. Data were collected at room temperature.

Surface Area Measurements. Surface area measurements were obtained with the BET method by using N_2 gas in an Omicron apparatus. Si-deposited substrates and plain substrates were heat treated to various temperatures prior to BET measurements in order to open up the pores and desorb H_2O.

NF_3 Decomposition. NF_3 decomposition was studied in an apparatus shown in Figure 2. A 1% NF_3 in He feed was used and He was also used as a potential diluent purge and carrier gas. Samples were loaded into a furnace and heated to various temperatures. The products of the decomposition were analyzed by gas chromatography (GC) methods using a thermal conductivity detector (TCD) and the effluents of the GC and the reactor were passed through a NaOH trap and then vented in a hood. Flow rates of 7.5 mL/min NF_3 in He were used. About 0.250 g of support or Si deposited support were used. The percent decomposition of NF_3 was determined chromatographically.

Results

Scanning Electron Microscopy. Scanning electron microscopy photos for Davisil and after CVD treatment at 800 °C on Davisil are shown in Figures 3a and 3b, respectively. The data of Figure 3a suggest that the particle size of Davisil before treatment is about 4–5 mm. After CVD treatment, data of Figure 3b show that the surface of the Davisil is coated with small fibers much smaller than 0.5 μm in size. A blowup of these

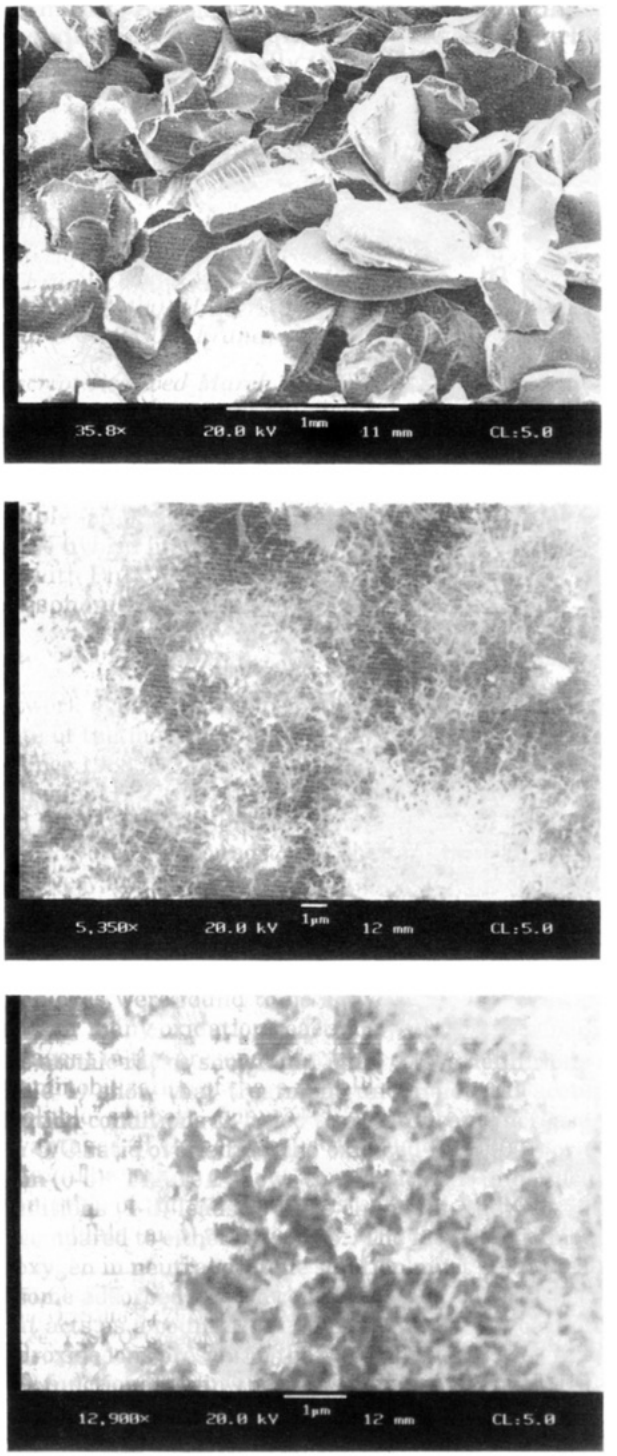

Figure 3. Scanning electron micrographs for (a, top) Davisil, (b, middle) Si/Davisil, 5350× magnification, and (c, bottom) Si/Davisil 12900× magnification.

fibers shown in Figure 3c, suggests that these whiskers are on the order of 0.1 μm.

Conditions used in the CVD reaction determine the resultant morphologies that are observed. For example, SEM data for samples treated at 900 °C shown in Figure 4a, at 1000 °C in Figure 4b, and at 900 °C in N_2 and H_2 in Figure 4c, show that different size particles are obtained at these different temperatures. Large fibers (5 μm long) appear at 900 °C; aggregation of particles (0.5–5 μm) occurs at 900 °C; and when N_2 and H_2 are used, very large particles on the order of 15 μm are observed.

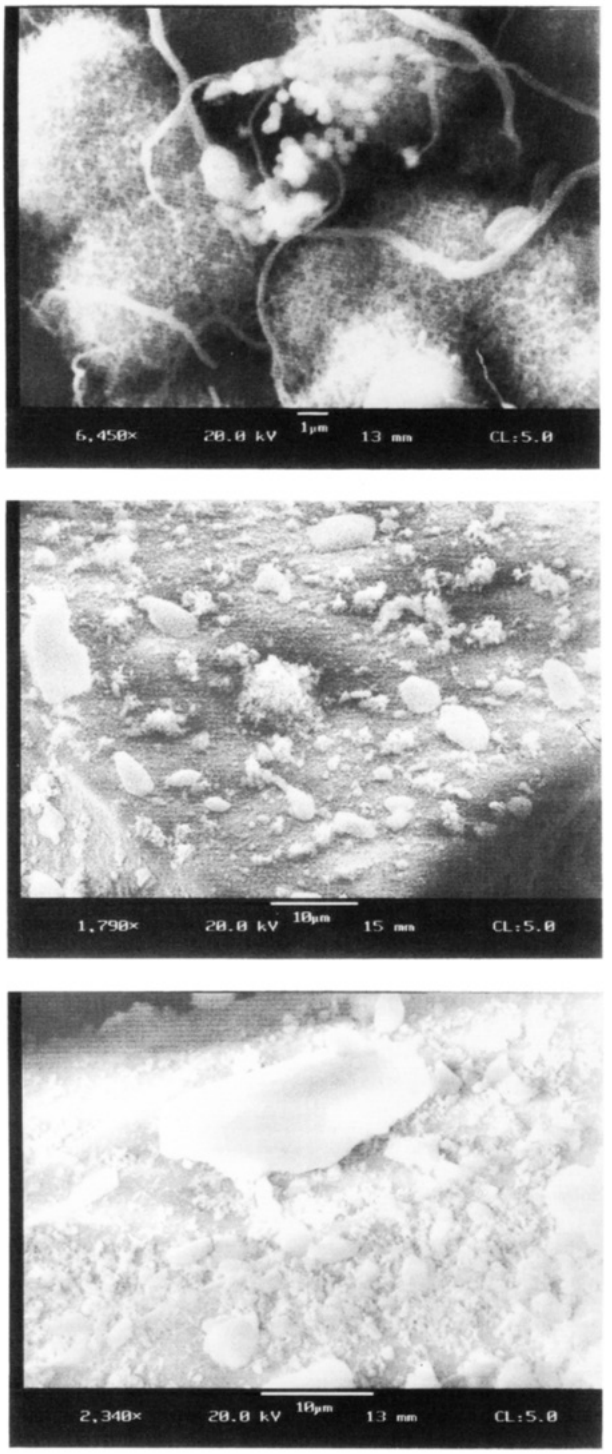

Figure 4. Scanning electron micrographs for (a, top) Si/Davisil, 900 °C, (b, middle) Si/Davisil, 1000 °C, and (c, bottom) Si/Davisil 900 °C, $H_2 + N_2$.

The nature of the porous substrate is also critical. For example, when a less porous Si gel is used instead of Davisil, SEM data of Figure 5a show that Si spheres on the order of 5 μm in diameter are formed in contrast to nanowhiskers of Figure 3b. Similar size spheres have been observed for CVD of Si on SiC fibers when $SiCl_4$ and H_2 are used.[37] In the case of AlN, clumps of fibers are produced as shown in Figure 5b.

X-ray Powder Diffraction. X-ray powder diffraction data for CVD treated Davisil at 800 °C and

(37) Hwan, L.; Willis, W. S.; Galasso, F. S.; Suib, S. L. *Adv. Ceram. Mater.* **1988**, *3*, 584–589.

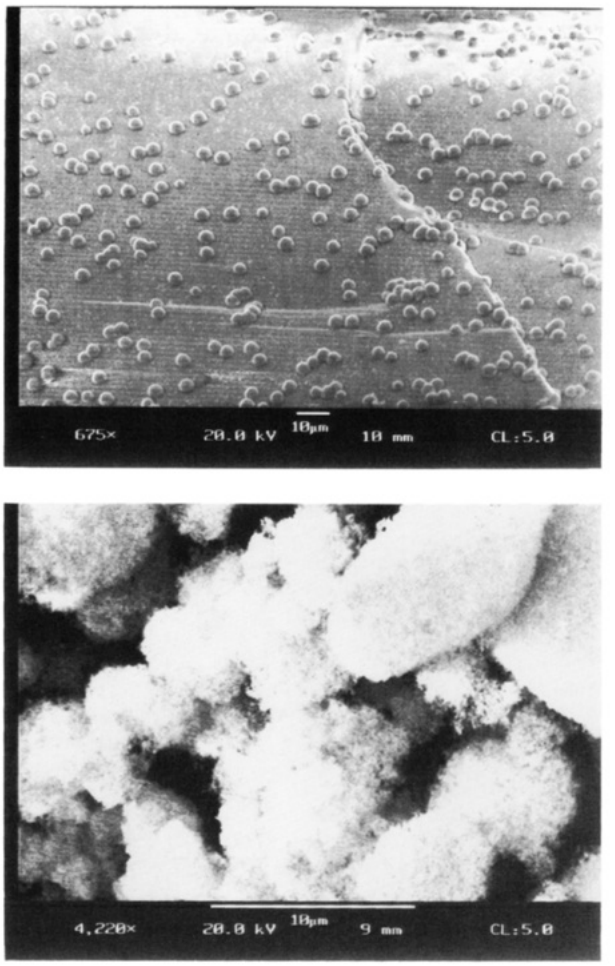

Figure 5. Scanning electron micrographs for (a, top) Si gel substrate and (b, bottom) AlN substrate.

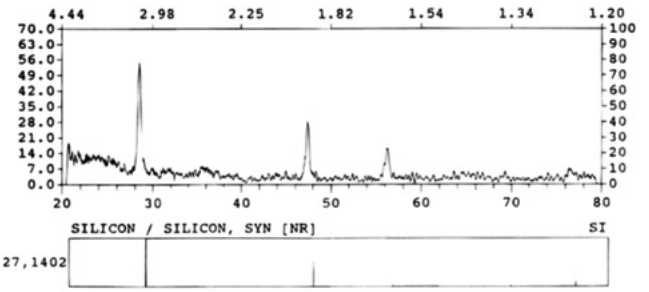

Figure 6. X-ray powder diffraction, Si/Davisil, 800 °C deposition.

standard stick patterns for Si, SiC, and C are shown in Figure 6. All three major lines for Si are observed in the CVD treated Davisil material, although the lines are broadened severely. Data for CVD treated AlN at 1050 °C are shown in Figure 7 along with standard data for AlN and SiC. Reflections indicative of both AlN and SiC are observed in these XRD data.

XRD data for CVD treated Davisil at 900 °C still show broad lines for Si as shown in data for lower temperature treatment (800 °C, Figure 6); however, a broad band between 31 and 39° 2θ appears that overlaps the three major lines for hexagonal SiC (h-SiC). For CVD treatment of Davisil at 1000 °C, distinct lines for SiC appear as well as the higher angle reflections (60, 72° 2θ) for SiC.

XRD data for CVD treated AlN materials at 800 °C showed no peaks. For carbon supports, XRD data show

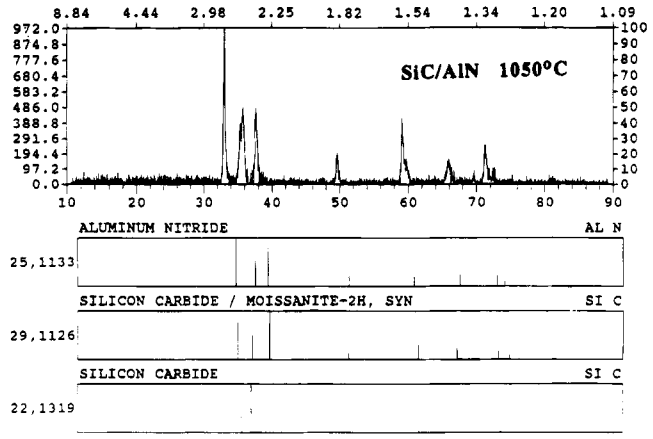

Figure 7. X-ray powder diffraction, Si/AlN, 1050 °C deposition.

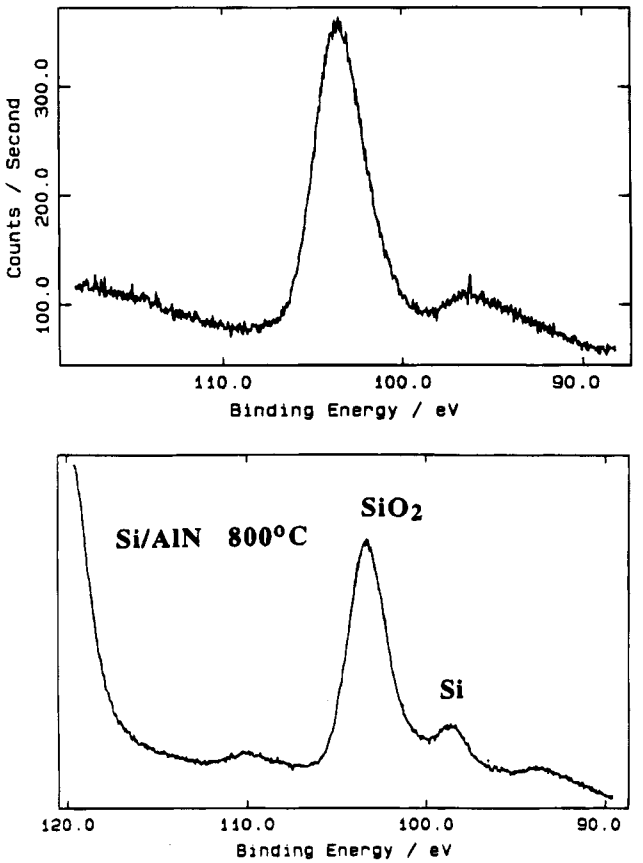

Figure 8. X-ray photoelectron spectroscopy, Si 2p region of (a, top) Si/Davisil, 800 °C deposition and (b, bottom) Si/AlN (800 °C deposition).

the presence of crystalline Si; however, the peaks are sharper than for Davisil supports. A summary of X-ray line broadening data is given in Table 1.

X-ray Photoelectron Spectroscopy. X-ray photoelectron spectroscopy data for the Si 2p region of CVD treated Davisil are shown in Figure 8a. A major peak at 103.6 eV is observed. There is an asymmetry to this peak with a very weak shoulder near 99 eV. XPS data for CVD treated AlN are shown in Figure 8b. In this case, the Si 2p region shows two distinct peaks, one at 103.3 eV and another at 99.1 eV. There is no difference in full width half-maxima for high- or low-resolution scans of the Si 2p region. Ar^+ ion sputtered materials show about the same fwhm (3.0 eV) as nonsputtered materials (3.1 eV). Peaks for Si, O, C, and Cl are observed for both substrates, and Al and N are also observed for the AlN substrate. The O/Si ratio decreases with sputtering from about 1.8 to 1.6. The surface $[Cl^-]$ is on the order of 2–4 atomic % in these materials.

Table 2. Surface Area Measurements

substrate	coating	heating temp[a]	surface area[b]
Davisil	none	RT	224
Davisil	none	900	185
Davisil	Si whiskers	900	189
AlN	none	1050	60
AlN	SiC	1050	55

[a] RT = room temperature; in °C. [b] In m^2/g.

Table 3. NF_3 Decomposition Data[a]

substrate	temp[b]	conversion[c]	products
Davisil	40	0	
	340	11.8	N_2
	375	43	NO, N_2
	480	98.7	NO, N_2, N_2O
Si powder[d]	47	0	
	280	3	N_2
	325	25.7	N_2
	355	35.2	N_2
	380	27	N_2
	450	99.5	N_2
Si whiskers/Davisil	40	0	
	200	2.4	N_2
	290	45.6	N_2
	345	100.0	N_2

[a] 1% NF_3, 7.7 mL/min, 0.25 g substrate. [b] In °C. [c] In %. [d] 40 μm.

Table 4. Gravimetric Data

sample	weight[a]	color
Davisil	0.2250	white
after Si deposition	0.2585	brown
after NF_3 reaction	0.2234	off-white

[a] In grams.

Surface Area Data. Surface area measurements with N_2 BET methods have been used to study the substrates before and after CVD treatment. A summary of BET data for the Davisil and AlN systems is given in Table 2.

NF_3 Decomposition. Data for NF_3 decomposition over Davisil, Si powder (40 μm diameter particles) and CVD treated Davisil are summarized in Table 3. Davisil starts to show activity near 340 °C, Si powder is active at 280 °C, and CVD treated Davisil is active at 200 °C. Davisil generates significant amounts of NO at 375 °C. The CVD treated Davisil shows some NO at 320 °C and N_2O at 480 °C. Si powder does not produce any oxides at any temperature. The temperature at which 100% conversion is reached for Davisil is 537 °C, for CVD-treated Davisil is 345 °C, and for Si powder is 450 °C.

Weight and color changes for Davisil after CVD treatment, and after reaction with NF_3 are summarized in Table 4. Note that before and after reaction that these materials are white or off-white in color whereas, CVD treatment leads to a grey-black color. After CVD treatment there is a 14.9% increase in weight. After reaction with NF_3, the weight is very similar to that before CVD treatment, and the color is off-white.

Luminescence. Luminescence emission data for CVD treated Davisil at various temperatures is given in Figure 9. The CVD treatment at 800 °C shows a very broad emission centered around 425 nm which extends

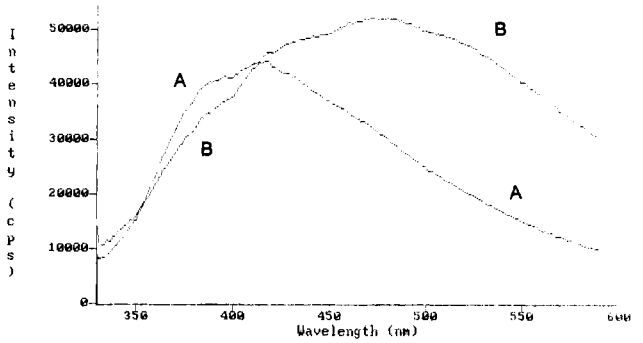

Figure 9. Luminescence emission spectrum of Si/Davisil, λ_{exc} = 310 nm, (A) 800 °C deposition and (B) 900 °C deposition.

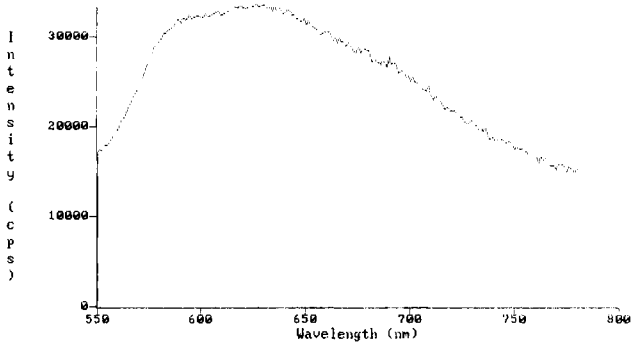

Figure 10. Luminescence emission spectrum of Si/NaY zeolite, λ_{exc} = 530 nm, 800 °C deposition.

beyond 600 nm. CVD treatment at 900 °C red shifts this emission with the most intensity occuring at 475 nm, with tailing at least to 700 nm. Similar luminescence emission data are given for another porous support, NaY zeolite, in Figure 10. In this case the emission maximum is near 625 nm with intensity out to at least 800 nm. The maximum wavelength for absorption in the Davisil system is about 310 nm, whereas the zeolite maximum excitation wavelength is about 530 nm.

Discussion

Generation, Structure, and Sizes of Si Whiskers. *Synthesis.* The XRD data of Figure 6 clearly show the formation of crystalline Si phase materials with Davisil and C substrates. Data for AlN substrates suggest that only amorphous materials are produced during CVD treatment at 800 °C. X-ray line broadening data of Table 1 for the crystalline Si nanowhiskers and the SEM data of Figure 3 suggest that 123 Å diameter materials form on Davisil during CVD treatment, whereas carbon substrates lead to 300 Å diameter whiskers and zeolite NaY leads to formation of 409 Å diameter whiskers.

XRD data of Figure 7, morphology data of Figures 3–5, line broadening data of Table 1, and surface area data of Table 2 clearly show that the nature of the substrate has a pronounced influence on the resultant materials that are deposited during CVD. XRD data of Figure 7 clearly show that under the same conditions that nanosize crystalline Si whiskers (Figure 3) are formed that amorphous materials having a more clumped morphology (Figure 5b) are formed on AlN. SEM data of Figure 4 show that as temperature is raised past 800 to 900 and to 1000 °C that the Si nanowhiskers start to aggregate. Use of a N_2/H_2 feed with methyltrichlorosilane also leads to aggregation and crystal growth. Si gel that is not as porous as Davisil leads to large spheres of Si (Figure 5a).

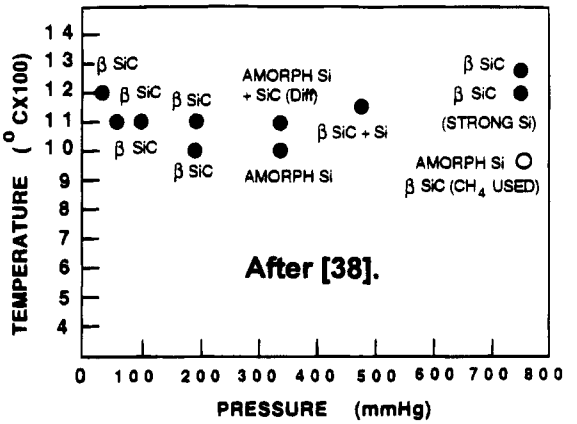

Figure 11. Phase diagram for various Si compounds based on experimental observations, after Veltri et al.

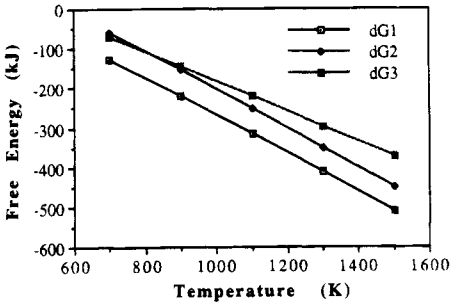

$SiCH_3Cl_3$ (g) ⟶ SiC (s) + 3 HCl(g) dG1

$SiCH_3Cl_3$ (g) ⟶ Si(s) + C(s) + 3 HCl(g) dG2

$SiCH_3Cl_3$ (g) + H_2(g) ⟶ Si(s) + CH_4(g) + 3 HCl(g) dG3

Figure 12. Thermodynamic calculations for Si formation.

XRD data for AlN substrate of Figure 7 and XRD data for CVD treatments at high temperature (900 °C and up) suggest that at elevated temperatures crystalline h-SiC formation is favored. A phase diagram for this system adapated from Veltri et al.[38] including the substrate work reported here is shown in Figure 11. It is clear that there exists a region of stability (see the open circle) for Si whiskers near 800 °C. Some thermodynamic calculations for this system with different products are summarized in Figure 12, again supporting our observation that Si can be produced under these conditions.

XPS data of Figure 8a suggest that the surface of the Si whiskers is oxidized. This is a reasonable observation, since oxygen affinity for Si surfaces is well known. The fwhm of the Si 2p region is so broad that this suggests there are at least two components contributing to this region. In the case of the AlN substrate, XPS data of Figure 8b clearly show that some of the surface exists as zerovalent Si. The reason why AlN appears to passivate the oxidation of Si nanowhiskers and why Davisil does not is not known with any certainty, however, the availability of oxygen sources (OH, O, H_2O) on Davisil is expected to be much greater than on AlN,

(38) Veltri, R.; Condit, D. A.; Galasso, F. S. *J. Am. Ceram. Soc.* **1989**, *72*, 478–480.

Table 5. Sizes of Coatings Produced by CVD Treatment of Methyltrichlorosilane and H_2

substrate	temp[a]	description	size
Davisil	800	fine whiskers	100 Å
Davisil	900	whiskers, fibers	<0.5 μm
Davisil	1,000	particles	<0.5 μm
SiO_2 Gel	800	spheres	3 μm
AlN	1,050	porous particulates	100 Å
MnO_2	820	porous spheres	<0.5 μm
TiO_2	800	particles, fibers	100 Å

[a] In °C.

Scheme 1. Synthesis of Si Whiskers and SiC on Davisil

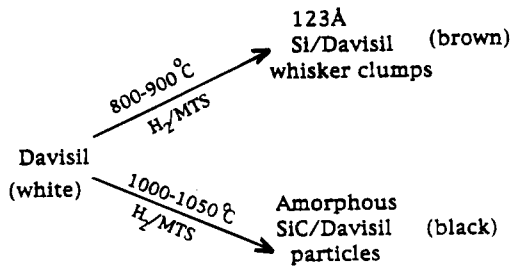

which has been proposed as a corrosion barrier in ceramic systems.[39,40]

The fact that oxidic substrates like Davisil and NaY zeolite show luminescence emission such as in Figures 9 and 10, respectively, may be related to the size of the Si whiskers, their degree of oxidation, and different functional groups that may exist on these materials. The differences in excitation wavelengths and emission maxima and broadness of the peaks may be related to Si/substrate interactions,[41] morphology,[42] quantum size effects,[43,44] and potential quenching effects[45] of different moieties in the substrates. Blue emission[46] as well as emission in the red region[41-45] of the spectrum have both been observed.

Cao and Hunt[49] have shown that for CVD deposited Si (around 150 Å particles) that as particle size increases a red shift in luminescence is observed. These data further corroborate our assertion that Si nanowhiskers smaller than the particulates reported by Cao and Hunt[49] are significantly shifted on Davisil supports. These data may have implications for the luminescence studies of porous Si materials that have recently been reported.[41-49]

A summary of different coating temperatures, morphologies, and sizes of particles is given in Table 5. A summary of the different stages of growth of Si materials with Davisil is given in Scheme 1 and for AlN and C in Scheme 2. Surface area data of Table 2 for Davisil

Scheme 2. Synthesis of Si Whiskers and SiC on AlN and C

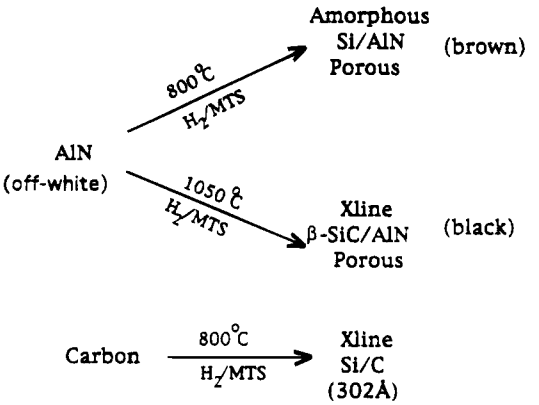

and AlN suggest that the pores of these materials remain open during the CVD process. It is plausible that the resultant distribution in sizes of Si nanowhiskers is related to a kind of shape-selective effect which is governed by the size and shapes of the pores of the substrates. The data appear to indicate that substrates having micropores of molecular dimensions such as zeolites and activated carbons produce larger diameter whiskers of Si than substrates like Davisil which has larger pores. Perhaps the rate of diffusion of Si precursors out of pores helps govern resultant sizes of whiskers. Further studies are underway in our laboratories to investigate this hypothesis.

NF_3 Decomposition. The NF_3 decomposition data provide further support that the predominant composition of the whiskers is indeed Si. The data of Table 3 clearly show that Si powder and Davisil treated by CVD are much more active at lower temperatures for NF_3 decomposition than the Davisil support itself. In general, we have found by studying a variety of metals and metal oxides that oxides promote production of NO and N_2O as is the case for Davisil alone, whereas metals and alloys only produce N_2 from NF_3. Only at elevated temperatures and when Si is depleted does the Si/Davisil material show signs of nitrogen oxides. Data of Table 3 also clearly show that highly dispersed Si is much more active at lower temperatures for NF_3 decomposition than larger particles of Si.

The weight change data of Table 4 also suggest that CVD of Si on Davisil provides active sites for NF_3 decomposition. After reaction, the weight returns to that before CVD treatment. Color changes are also in line with these suggestions. Analysis of the materials collected before traps suggest that SiF_4 is the major initial product from reaction of F of NF_3 with the Si whiskers. The SiF_4 then goes on to be hydrolyzed in the trap.

Conclusions

We have shown here that CVD methods can be used to produce Si nanowhiskers over a variety of porous supports. Certain supports allow formation of smaller whiskers than others. Nanowhiskers ranging between 123 and 300 Å diameters have been observed. Characterization of the Si whiskers has been done with X-ray, line broadening, SEM, XPS, and luminescence methods. The smallest diameter Si whiskers are most active as getters in the decomposition of NF_3. The porosity of the substrate is clearly an important factor

(39) Bertolet, D. C.; Liu, H.; Rogers, J. W. *Chem. Mater.* **1993**, *5*, 1814-1818.
(40) (a) Tan, B. J.; Xiao, Y.; Suib, S. L.; Galasso, F. S. *Chem. Mater.* **1992**, *4*, 648-657. (b) Xiao, Y.; Tan, B. J.; Suib, S. L.; Galasso, F. S. U.S. Patent 5,279,808.
(41) Wallich, P. *Sci. Am.* **1993**, *269*, 22-23.
(42) Kang, Y.; Jorne, J. *J. Electrochem. Soc.* **1993**, *140*, 2258-2265.
(43) Sagnes, I.; Halimaoui, A.; Vincent, G.; Badoz, P. A. *Appl. Phys. Lett.* **1993**, *62*, 1155-1157.
(44) Koos, M.; Pocsik, I.; Vazsonyi, E. B. *Appl. Phys. Lett.* **1993**, *62*, 1797-1799.
(45) Lauerhaas, J. M.; Sailor, M. J. *Science* **1993**, *261*, 1567-1568.
(46) Lee, M. K.; Peng, K. R. *Appl. Phys. Lett.* **1993**, *62*, 3159-3160.
(47) Chun, J. K. M.; Bocarsly, A. B.; Cottrell, T. R.; Benziger, J. B.; Yee, J. C. *J. Am. Chem. Soc.* **1993**, *115*, 3024-3025.
(48) Sham, T. K.; Jiang, D. T.; Coulthard, I.; Lorimer, J. W.; Feng, X. H.; Bryskiewicz, B. *Nature* **1993**, *363*, 331-334.
(49) Cao, W.; Hunt, A. J. *Appl. Phys. Lett.* **1994**, *64*, 2376-2378.

in formation of Si whiskers, although there are other important factors such as composition, size, and shape of the pores, and hydrophilicity. The ability to produce aligned Si whiskers on thin-film surfaces in specific orientations is a related area that may be important in electronic and semiconductor applications. In addition, the ability to deposit nanosize Si whiskers on semiconducting substrates such as TiO_2, SiC, Si, and other materials may allow a broadening of the absorption capacity of such systems for photocatalytic applications.

Acknowledgment. We thank United Technologies Research Center for support of this research. We thank Mike LeClaire for making surface area measurements.

CM940565S